CO oxidation by rutile TiO2(110) doped with V, W, Cr, Mo, and Mn

ARTICLE *in* THE JOURNAL OF PHYSICAL CHEMISTRY C · JULY 2008

Impact Factor: 4.77 · DOI: 10.1021/jp802296g

CO Oxidation by Rutile TiO_2(110) Doped with V, W, Cr, Mo, and Mn

Hyun You Kim,[†,‡] Hyuck Mo Lee,[‡] Raj Ganesh S. Pala,[†] Vladimir Shapovalov,[§] and Horia Metiu*[,†]

Department of Chemistry and Biochemistry, University of California, Santa Barbara, California 93106, Department of Materials Science and Engineering, KAIST, 335 Gwahangno, Yuseong-gu, Daejeon 305-701, Korea, and Department of Chemical Engineering, University of California, Berkeley, California 94720-1462

Received: March 17, 2008; Revised Manuscript Received: May 9, 2008

We used density functional theory to study CO oxidation catalyzed by TiO_2(110), in which some Ti atoms on the surface are replaced with V, Cr, Mo, W, or Mn. We find that in the presence of O, V, Cr, Mo, and W dopants at the surface bind an oxygen atom so that the dopant has formula MO (M = V, Cr, Mo, W). Rutile doped with Mn does not take an oxygen atom from the gas phase. We find that these materials oxidize CO by a Mars−van Krevelen mechanism in which the role of the dopant is to facilitate the formation of oxygen vacancies. The energy of CO reaction with an oxygen atom from the surface layer decays linearly with the energy of vacancy formation ΔE_v, whereas the energy of adsorption of O_2 at a vacancy is a linear function of ΔE_v. These are the only two reactions in the mechanism whose energy varies from one doped oxide to another. Because they both depend on the energy of oxygen vacancy formation, the latter quantity is a good descriptor of catalytic activity. In deciding which intermediate reactions are most likely from an energetic point of view, we impose a "spin conservation" rule: a reaction that requires "flipping a spin" is too slow for catalysis. Because of this, we only consider reactions that conserve spin. We find that all the dopants studied here lower the energy of vacancy formation; therefore, the doped oxides are better oxidants than the undoped ones.

1. Introduction

There are indications, from theory and experiment, that substitutionally doped oxides might be a class of interesting partial oxidation and oxidative dehydrogenation catalysts. The explicit idea of using doped oxides (or mixed oxides as they were called in the older literature) seems to go back to Cimino and co-workers,[1,2] who showed that $Ni_xMg_{1-x}O$ is more active for N_2O decomposition than NiO. Although doped oxides received some attention in the older literature,[3,4] there have been few studies of their catalytic activity. The only review article we could find[5] was written in 2002 and contains only a few examples. There are recent papers[6–13] proposing that the catalytic activity of certain metal-on-oxide catalysts is due to the ionic form of the metal; for example, the active catalytic centers in the Au/ceria catalyst for the water-gas shift reaction or CO oxidation are Au ions. These papers are somewhat controversial because the proof that the catalyst is ionic is indirect, and there is also the possibility that small, undetected neutral clusters are responsible for the catalytic activity.

More important to us are papers that set out to prepare doped oxides to use as catalysts or to make the host oxide a better oxidant.[1,2,13–44] Most among these papers found that doping lowers the temperature at which the oxide is reduced by CO or H_2. Those who studied a catalytic reaction found that doping improves the catalytic activity of the host oxide. Thus, $Cu_xCe_{1-x}O_2$ was used for NO reduction with NH_3 or CO;[45] $Pt_xCe_{1-x}O_2$, $Rh_xCe_{1-x}O_2$, and $Ti_xCe_{1-x}O_2$ for CO oxidation;[18,20,46] $Fe_xCe_{1-x}O_2$ for N_2O decomposition;[22] $Ce_{0.9}Cu_{0.1}O_2$ for steam reforming of methanol;[25] TiO_2 doped with Li, Na, K, Cs catalyzes acetone oligomerization;[28] $Pt_xCe_{1-x}O_2$ catalyzes methane oxidation to H_2 and CO; and $Sm_{0.8}Sr_{0.2}O_x$ and $La_{0.98}Sr_{0.02}O_x$ catalyze the oxidative dehydrogenation of propane and ethane to propene, ethylene, and methane.[36] The oxidative dehydrogenation of alkanes by Li doped MgO[30–35,37–44] has also been studied extensively. In all these examples the activity of the doped oxide was higher than that of an undoped one.

Doping is not always beneficial. Ceria doped with Sm, Gd, La, Nb, and Ta has lower activity toward n-butane oxidation[47] than ceria alone, and doping ceria with La, Pr, Gd, or Nb slows down CO oxidation.[27]

A group at Daihatsu Motors and Cataler Corporation found[14–17] that the doped perovskite $LaFe_{0.95}Pd_{0.05}O_3$ has better catalytic properties and higher thermal stability than the conventional automotive exhaust catalyst of Pd-metal clusters supported on alumina.

These articles suggest that doped oxides might be a promising class of catalysts. Considering that a large number of oxides can be combined with a large number of dopants and considering the large number of oxidation and oxidative dehydrogenation reactions that might be catalyzed by such compounds, we feel that the potential of this class of catalyst has not been fully explored by either theory or experiment. This prompted us to use density functional theory (DFT) to examine several doped oxides to determine the extent to which they might be good oxidation catalysts. Our premise was that in many systems the presence of a well-chosen dopant weakens the bond of the neighboring oxygen atoms to the surface and increases their chemical activity. Therefore, such a doped oxide is a better oxidant than the undoped one, and it is more likely to engage in an oxidation reaction by a Mars−van Krevelen mechanism in which a surface oxygen atom oxidizes a reagent and is

* E-mail: metiu@chem.ucsb.edu; fax: 805-893-4120; phone: 805-893-2256.
† University of California, Santa Barbara.
‡ KAIST.
§ University of California, Berkeley.

10.1021/jp802296g CCC: $40.75
Published on Web 07/17/2008

removed from the surface leaving behind an oxygen vacancy. If the dopant concentration is low and the dopants are spatially separated, one expects that removal of one oxygen atom in the neighborhood of a dopant will make it harder to remove a second atom. There is, thus, a temperature window in which the system will provide only one oxygen atom per dopant, which means that one might achieve selective partial oxidation.

A better oxidant is not necessarily a better oxidation catalyst. The oxidation reaction creates oxygen vacancies on the surface, and to close the catalytic cycle these vacancies must be healed by gas phase oxygen. Because an O_2 molecule provides two oxygen atoms, and only one is needed for annihilating the vacancy, a mechanism must be found for using the superfluous oxygen atom. In the case of CO oxidation by rutile $Au_xTi_{1-x}O_2$ (110)[48] and by $Au_xCe_{1-x}O_2$ (111),[49] we found that O_2 adsorbs at the oxygen vacancy site and that its O−O bond is weakened by contact with the electron rich vacancy. CO reacts with this activated O_2 to form a "carbonate" that easily decomposes to release CO_2 and heal the oxygen vacancy. This restores the surface to its initial state and completes the catalytic cycle.

The formation and the annihilation of the oxygen vacancies are critical steps in this Mars−van Krevelen mechanism, and this suggests that the energy of vacancy formation (ΔE_v) might be a good "descriptor" of the catalytic properties of doped oxides. Doped oxides that form oxygen vacancies very readily are good oxidants but they are not necessarily good oxidation catalysts since the reduced surface is not likely to be easily reoxidized. On the other hand, if the energy required for making oxygen vacancies is too high, then the system is not a good oxidant and is therefore not a good catalyst. One anticipates that a plot of the catalytic activity versus the energy of vacancy formation will have a maximum (similar to the famous "volcano curve" in other systems). The activity will peak at an optimal value of ΔE_v where vacancy formation is not too hard and not too easy.

As Norskov's work has shown,[50–54] finding a simple descriptor of a complex catalytic mechanism is extremely helpful for a preliminary screening aimed at finding the best system, for a given reaction, in a class of catalytic materials. We hope that the energy of oxygen vacancy formation will provide such a criterion for partial oxidation reactions by doped oxides.

Our work has shown[48,55] that doping rutile TiO_2 (110) with Ru, Sn, Mn, Ni, Pd, Pt, Cu, Ag, or Au substantially lowers the energy of oxygen vacancy formation, whereas doping with Zr and Hf causes practically no change. Doping CeO_2 (111) with Au, Cu, and Ag also lowers the energy of vacancy formation. However, this effect is not universal;[56] doping ZnO ($10\bar{1}0$) with Sc, Y, La, Ti, Zr, Hf, Ce, V, Nb, or Ta very substantially increases the energy of vacancy formation. All these dopants have higher valence than the Zn atom they substitute, and they bind the oxygen atoms near them more strongly, making them less likely to engage in oxidation chemistry. In the present article we investigate whether this is true for rutile TiO_2 (110) doped with high valence atoms such as Cr, Mo, W, Mn, and V.

Because we are interested in using these doped oxides as oxidation catalysts, we need to know their structure in the presence of gas-phase oxygen. We found that at all reasonable oxygen pressures and temperatures V, Cr, Mo, and W will bind an oxygen atom from gas phase to form a compound that we denote by $(MO)_xTi_{1-x}O_2$ (110), with M = Cr, Mo, W, or V. The manganese doped oxide does not bind oxygen from the gas phase and prefers to exist as $Mn_xTi_{1-x}O_2$ (110).

Our calculations find that the energy of oxygen vacancy formation in $(MO)_xTi_{1-x}O_2$ (110)—with M = V, W, Cr, or Mo—and in $Mn_xTi_{1-x}O_2$ is smaller than in TiO_2 (110). This behavior is different from what we have expected by extrapolating the results obtained[56] for ZnO. Perhaps this happens because Ti and the dopants considered here are capable of taking a variety of valence states and can therefore adapt to the changes in their environment introduced by doping. Zn does not have this ability, therefore the Zn atoms in ZnO do not adjust when their environment is disrupted by doping. Our calculations also find that the energy of oxygen vacancy formation in $(MO)_xTi_{1-x}O_2$ (110) is smaller than that of $M_xTi_{1-x}O_2$ (110) (for M = V, Cr, Mo, or W). This is not surprising; if the dopant binds an additional oxygen atom, then we expect its bond to the other oxygen atoms in the surface to weaken so that it is easier to remove one of them from the surface.

The mechanism of CO oxidation by $(MO)_xTi_{1-x}O_2$ (110) (for M = V, Cr, Mo, or W) is similar to that observed on $Au_xTi_{1-x}O_2$ (110)[48] and $Au_xCe_{1-x}O_2$ (111):[49] (1) CO adsorbs and "reacts" with two oxygen atoms on the surface to form a "carbonate"; (2) the carbonate decomposes easily to release CO_2 in the gas phase and form an oxygen vacancy on the surface; (3) O_2 adsorbs at the oxygen vacancy site, and its O−O bond is weakened by interaction with this electron rich environment; (4) the adsorbed O_2 reacts with CO to form a carbonate; and (5) the carbonate decomposes to produce gas phase CO_2 and heal the oxygen vacancy. For $(VO)_xTi_{1-x}O_2$ (110) this completes the catalytic cycle; the surface after step 5 is the same as the surface prior to step 1. However, the story does not end here for $(MO)_xTiO_{1-x}$ (110) with M = Cr, Mo, or W. For these compounds the spin state of the surface after step 5 is different from the spin state prior to step 1. It takes a second cycle of the same reactions (but with different spin states) for the surface to return to the spin state it had at the beginning. We are not aware of another example of such behavior in the literature.

The $Mn_xTi_{1-x}O_2$ (110) behaves differently in two respects; in step 1 CO reacts with one oxygen atom on the surface to form a complex that closely resembles a CO_2 molecule stuck in an oxygen vacancy; and the spin state after step 5 is the same as the spin state prior to step 1.

A surprising finding is that the energy of the reactions 2, 4, and 5 are independent of the nature of the catalyst. In addition, the energy of the adsorption of CO to the doped oxide (step 1) and the energy of adsorption of O_2 at the vacancy site (step 3) are linear functions of ΔE_v. Therefore, it appears that ΔE_v is a useful descriptor of two of the steps in the catalytic process.

We end with a word of caution. The method by which we take into account the role of spin is reasonable, but it is not a well-defined approximation within the framework of a rigorous theory. It needs to be tested further against experiments and better theoretical methods. It also appears that DFT does not accurately describe the energetics of oxygen vacancy formation[57] and the chemistry of doped oxides[58,59] for narrow band oxides such as TiO_2. It is unclear at present for which systems such errors exist, how large they are, or which quantities are described erroneously. However, we are interested here in qualitative questions: (1) is the energy of vacancy formation a good qualitative descriptor of oxidation catalysis by the Mars−van Krevelen mechanism? (2) Which doped oxide is a better catalyst? (3) Is there a wide variability in the chemistry of doped oxides (which would indicate that a study of various dopants is worthwhile)? We assume that DFT is able to answer these qualitative questions reliably if not accurately (i.e., a better catalyst in a DFT calculation should be a better catalyst in reality). One should also keep in mind that the perfect crystal slabs studied by theory are a questionable model of real catalysts

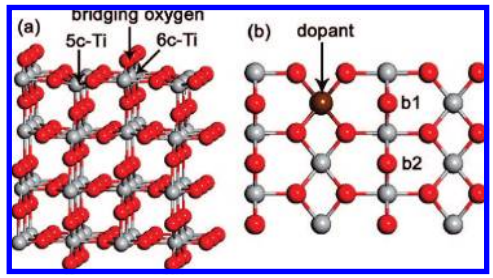

Figure 1. The [3 × 2] slab used for DFT calculations; a side view (left) and a view of the top layer (right). The bridging oxygen atoms, the five coordinated titanium atoms (5c-Ti), and the six coordinated titanium atoms (6c-Ti) are marked in the figure. One of the 5c-Ti atoms is replaced by a dopant. We replace 16.6% of the titanium atoms in the surface layer. The 1st and 2nd nearest bridging oxygen atoms from the dopant are labeled b1 and b2, respectively. The red sphere are the oxygen atoms, the gray ones are the Ti atom, and the brown ones are the dopant.

that are often amorphous and have an extremely complicated, ill defined, and unknown structure. Even if we had a very accurate theory, it would only solve accurately for the properties of inaccurate models of the catalyst. Given this situation, we prefer to think of the theory as a qualitative tool that may help us guess which systems are most likely to be useful catalysts.

2. Computational Method

We performed spin-polarized Kohn−Sham DFT calculations with plane-wave VASP code[60–63] and the Perdew−Wang functional.[64,65] The ionic cores are described by the PAW method implemented in VASP.[60–63]

To describe the surface we used a rutile TiO_2 (110) slab having 12 atomic layers and a surface supercell of [3 × 2] (see Figure 1). The surface energy of rutile TiO_2 slab and the binding energy of molecules to the surface depends on slab thickness,[66–70] however it appears that these quantities are converged if we use 12 atomic layers and fix the atoms in the bottom six layer in the bulk positions.[57,67] The atomic positions in the top 6 layers were allowed to relax during geometry optimization. Because of the large size of the supercell, the energy was calculated only at the Γ-point. The plane wave energy cutoff was 263.7 eV, when rutile was doped with V, Mo, or W, and 300.0 eV when the dopant was Mn or Cr. The convergence criteria for the electronic wave function and for the geometry were 10^{-5} and 10^{-4} eV, respectively. We used the Gaussian smearing method with initial window size of 0.02 eV, which was gradually decreased down to 0 during geometry optimization, to prevent partial occupancy. In each calculation involving the doped oxide, one out of the six 5-coordinated Ti atoms (5c-Ti) in the surface layer was replaced with a dopant (V, Mn, Cr, Mo, or W) (see Figure 1).

After doping, oxygen was allowed to react with the dopant and to oxidize the doped oxide. We found three bound states: one in which an oxygen atom is bonded to the dopant and two in which an O_2 molecule is adsorbed at the dopant site (see Figure 2). The energy of formation of the oxidized doped oxide is given by eq 1.

$$E = E_{odo} - E_{do} - {}^{n}/_{2}E(O_2(g)) \quad (1)$$

Here, E_{odo} is the energy of the oxidized doped oxide slab, n is the number of bonded oxygen atoms, E_{do} is the energy of the doped oxide slab, and $E(O_2(g))$ is the energy of the gas phase oxygen molecule (calculated with DFT).

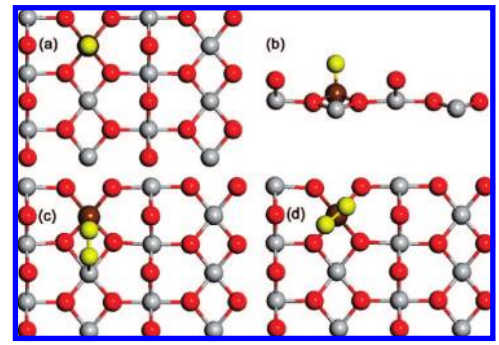

Figure 2. The structure of the oxidized doped oxide surface. (a) An oxygen atom adsorbed on top of the dopant (top view). (b) The side view of the oxygen atom adsorbed on top of the dopant. (c) An O_2 molecule adsorbed in a bridging position on the dopant (labeled MO_2). (d) An O_2 molecule adsorbed at the side of the dopant (labeled MO_2'). The brown sphere represents the dopant, the magenta spheres are the oxygen atoms that are not part of the oxide surface, the red spheres are the oxygen atoms belonging to the oxide surface, and the gray spheres are the Ti atoms.

The binding energies are used to calculate the composition of the oxidized surface when the doped oxide is in equilibrium with gaseous oxygen. For this we need to know the chemical potential of the species that form when the doped oxide is exposed to oxygen. We use an ideal lattice−gas model to find the chemical potential of the adsorbed oxygen species and the vibrational energies calculated by DFT. The lattice−gas model is valid at low dopant concentration, which is the case interesting in practice. To limit the computational cost, vibrational analysis was performed by displacing only the atoms bounded to dopant (M). This means that we consider in the thermodynamic calculations only the vibrational modes localized on the dopant and disregard the phonons. We assume that in the equilibrium calculations the phonon contribution from the reactants cancels that from the products.

Quantum mechanics requires that, in the case when spin−orbit coupling is small, the electronic wave function must be an eigenstate of the total spin operator squared (S^2). In addition, reactions in which the total electron spin of the reactants is different from the total electron spin of the products are slow.[71–80] With few exceptions,[81–83] these "spin conservation" rules have been ignored in catalysis studies. In this article we implement them as follows.[84] We use spin-polarized DFT to calculate the spin−orbitals of the system. We place the electrons in these orbitals so that the spin polarization N_s has a certain value (N_s is the absolute value of the number of spins up minus the number of spins down). We optimize the energy and the structure by holding N_s fixed. Different energies and atomic positions are generated for different values of N_s. We identify the total spin quantum number to be $S = N_s/2$ and the spin multiplicity to be $N_s + 1$. When the system consists of two separated parts (e.g., an O_2 in the gas phase and the surface) having the spins S_1 and S_2, we calculate the total spin S of the system by using the spin addition rule: S can be any of the values $|S_1 - S_2|$, $|S_1 - S_2| + 1$, $|S_1 - S_2| + 2$..., $S_1 + S_2$. For example, when O_2, which is a triplet ($N_s = 2$, $S_1 = 1$), adsorbs on a surface that is a triplet ($N_s = 2$, $S_2 = 1$), then the total spin of the system is one of 0, 1, or 2. The adsorption of O_2 on the surface is allowed in one of these states. For thermodynamic studies we choose the spin state that has the lowest energy. This method is an "improvisation" rather than a theory and needs to be tested further. It is similar (except in some details) to the method used by Behler et al.,[81,82] which seems to successfully explain the strange behavior of O_2 adsorption on Al. We have

TABLE 1: The Energies of Formation of the Compounds Shown in the First Column[a]

	dopant			
energy of formation	V (eV)	Cr (eV)	Mo (eV)	W (eV)
$(MO)_xTi_{1-x}O_2$ (110)	−0.94	−0.90	−3.02	−3.75
$(O_2)_xM_xTi_{1-x}O_2$ (110)	−0.46	−0.12	−1.98	−2.79
$(O_2')_xM_xTi_{1-x}O_2$ (110)	−0.40	−0.23	−2.42	−3.12

[a] These are the energies of the reactions $^1/_2O_2 + M_xTi_{1-x}O_2$ (110) = $(MO)_xTi_{1-x}O_2$ (110) (first row of numbers), $O_2 + M_xTi_{1-x}O_2$ (110) = $(O_2)_xM_xTi_{1-x}O_2$ (110) (see the structure in Figure 2c) in the second row, and $O_2 + M_xTi_{1-x}O_2$ (110) = $(O_2')_xM_xTi_{1-x}O_2$ (110) (see the structure in Figure 2d) in the third row. The manganese dopant does not adsorb oxygen.

also shown[55] that it gives satisfactory results for O_2 dissociation at an oxygen vacancy site on rutile TiO_2 (110), whereas DFT without imposing spin conservation[67,85] gives results in disagreement with experiment.[86,87]

Finally, the Bader charges[88] reported in this article were calculated by using the method of Henkelman, Arnaldsson, and Jonsson.[89]

3. The Structures and the Energies of the Oxidized Doped Surfaces

All dopants used here are capable of having a valence higher than four. Therefore, it is possible that their "desire" to bind to oxygen is not wholly satisfied when they replace a Ti^{IV} atom in TiO_2. This means that these dopants might bind more oxygen if they are exposed to O_2. We found that Mn does not bind any extra oxygen atom, but the other dopants (V, Cr, Mo, or W) form the three oxygenated compounds shown in Figure 2 and labeled MO, MO_2, and MO_2' (M could be V, Cr, Mo, or W). Among these, MO has the highest formation energy (see Table 1). The formation energies were calculated using those spin states that have the lowest energy. We did this because we assume that during the preparation of the oxygenated doped surface the solid will be exposed to oxygen for a long time. This means that the spin−orbit coupling will have a chance to bring the system into the spin state having the lowest energy.

It is common, but incorrect, to assume that the compound having the lowest energy is the most stable. The correct procedure for finding the concentration of these oxygenated compounds on the surface uses the equilibrium condition involving the chemical potentials of the reaction participants.[90] Using energy as a criterion is valid only when the energies being compared are very different. In our case, energy-based conclusions are safe for Cr, Mo, and W. However, for V the difference in energy of formation of $(VO)_xTi_{1-x}O_2$ (110) and that of $(O_2)V_xTi_{1-x}O_2$ (110) is fairly small. Because of this, we have calculated the vibrational frequencies of VO and the adsorbed O_2 and have used a lattice gas model to compute the chemical potential of the oxygenated doped oxide. The gas phase chemical potential of oxygen can be easily calculated.[91] This information can be used in the equilibrium conditions to determine the equilibrium concentration[90] of $(VO)_xTi_{1-x}O_2$ (110), $(O_2)V_xTi_{1-x}O_2$ (110), and $(O_2')V_xTi_{1-x}O_2$ (110) as a function of temperature and oxygen pressure. We found that at all temperatures of interest to experiments and at an oxygen pressure of 1 atm, the only surface species at equilibrium is $(VO)_xTi_{1-x}O_2$ (110). Because of this, we examine in what follows only the catalytic activity (for CO oxidation) of $(MO)_xTi_{1-x}O_2$ (110) (M = V, Cr, Mo, or W) and of $Mn_xTi_{1-x}O_2$ (110).

TABLE 2: The Energy Required for Removing an Oxygen Atom from the b2 Position (see Figure 1) to Form $^1/_2O_2$ in the Gas Phase[a]

	ΔE_{v2} (eV)	$2S + 1$
$V_xTi_{1-x}O_2$	3.37	2
$(VO)_xTi_{1-x}O_2$	1.53	2
$Cr_xTi_{1-x}O_2$	2.67	3
$(CrO)_xTi_{1-x}O_2$	1.91	1
	1.73	3
$Mo_xTi_{1-x}O_2$	3.49	3
$(MoO)_xTi_{1-x}O_2$	2.97	1
	1.71	3
$W_xTi_{1-x}O_2$	3.61	3
$(WO)_xTi_{1-x}O_2$	3.49	1
	1.97	3
$Mn_xTi_{1-x}O_2$	2.31	4

[a] The energy for removing an oxygen atom from b1 is larger, and CO binds more strongly to the oxygen atom b2; this is why we do not give ΔE_{v1}. $2S + 1 = N_s + 1$ is the spin state of the system prior to the removal of the oxygen atom.

4. The Energies of Oxygen Vacancy Formation in $(MO)_xTi_{1-x}O_2$ (110) (M = Mo, Cr, W, or V) and $Mn_xTi_{1-x}O_2$ (110)

We assume that materials that form oxygen vacancies more easily are better oxidants. If true, this provides us with a simple descriptor of the oxidizing power of an oxide (doped or otherwise). The oxygen atoms b1 and b2 in Figure 1 are the ones most affected by the presence of the dopant. We denote by ΔE_{vi} (i = 1, 2) the energy needed for removing an oxygen atom from bi, to form $^1/_2O_2$ in the gas phase and creating an oxygen vacancy on the surface of $M_xTi_{1-x}O_2$ (110). For all systems studied here (and for the ones studied previously[48]), $\Delta E_{v2} < \Delta E_{v1}$. We conjecture that the oxygen at b2 binds CO more strongly, and the calculations show that this is the case. The values of ΔE_{v2} are given in Table 2 for all the spin states involved in the catalytic oxidation of CO. Both ΔE_{v2} and ΔE_{v1} are lowered by doping with M (M = V, Mo, Cr, or Mn) and are lowered further when doped with MO (M = V, Mo, Cr, or W). In our previous work[48,49,56] we have found the following propensity rule: dopants having a lower valence than the cation they are replacing in the oxide will make it easier to make oxygen vacancies; those that have a higher valence will make it harder. The results presented in Table 2 do not abide by this rule; V, Cr, Mo, Mn, VO, MoO, WO, and CrO dopants lower the energy of vacancy formation.

It is difficult to understand the reason for this behavior. Intuitively, one would expect that a dopant having a higher valence than the atom it replaces is under-coordinated and will tend to more strongly bind the neighboring oxygen atoms. This is the case for doped ZnO.[56] The systems examined here differ from ZnO in one respect: Ti is capable of having a variety of valence states and therefore can readily adjust to accommodate unusual coordination. The dopants have the same capability. Table 3 shows the formation enthalpies of MO_2 (M = Ti, V, Cr, Mo, W, and Mn) oxides and the most stable M oxides. Vanadium forms[92] VO, V_2O_2, V_3O_4, V_2O_3, V_3O_5, VO_2, V_2O_4, V_6O_{13}, and V_2O_5, and the heat of formation of VO_2 is a bit smaller than the heat of formation of rutile TiO_2. We expect, therefore, that doping TiO_2 with V does not radically change the energy of oxygen vacancy formation; indeed, the change is from 3.57 to 3.37 eV, which is a small amount compared to most other dopants. Chromium forms CrO, Cr_2O_3, CrO_2, and CrO_3, among which Cr_2O_3 has the highest heat of formation (CrO_2 has the rutile structure but it less stable than Cr_2O_3).

TABLE 3: Formation Enthalpies for MO_2 and the Most Stable M Oxides[a]

M	$\Delta H°(MO_2)$, kJ/mol	highest enthalpy of formation	$\Delta H°_{max}$, kJ/mol	ΔE_{v2}(M), eV	electron config.
Ti	−941	TiO_2 (rutile)	−941	3.72	$3d^24s^2$
V	−715	V_2O_5	−779	3.37	$3d^34s^2$
Cr	−590	CrO_2	−590	2.67	$3d^54s^1$
Mo	−589	MoO_3	−754	3.49	$4d^55s$
W	−570	WO_3	−840	3.61	$5d^46s^2$
Mn	−521	MnO_2	−521	2.31	$3d^54s^2$

[a] Column 2 contains the standard enthalpies of formation of the MO_2 oxide (M = Ti, V, Cr, Mo, W, Mn) per metal atom. Column 3 gives the oxide having the highest enthalpy of formation per cation. Column 4 gives the highest enthalpy of oxide formation per cation. Column 5 gives the energy of oxygen vacancy formation (one vacancy and 1/2 O_2 in the gas phase) for the $M_xTi_{1-x}O_2$ (M= Ti, V, Cr, Mo, W and Mn). The last column gives the electronic structure of the dopant and of Ti atoms.

Therefore, it seems reasonable to assume that Cr would attempt to take a formal charge of +3, but it has difficulty doing so because the oxygen atoms surrounding it have rutile structure and therefore are located in the "wrong" position. This is why Cr bonds with the oxygen in the rutile TiO_2 are weaker than that of Ti and making an oxygen vacancy is easier in the doped oxide. Mo forms MoO_2 with a rutile structure and also MoO_3, Mo_4O_{11}, Mo_8O_{23}, and Mo_9O_{26}. Among these oxides, MoO_3 has the highest heat of formation per molybdenum atom, and the heat of formation of MoO_2 is less than that of TiO_2. Thus, Mo prefers not to form Mo^{IV}, and if it is forced to do so it would not bind oxygen as strongly as the Ti atom it replaces. Hence, doping with Mo or MoO will make it easier to remove an oxygen atom from the surface of the oxide. Manganese forms MnO, Mn_3O_4, Mn_2O_3, and MnO_2, the last three having two isomorphs each. β-MnO_2 has rutile structure, and it has the lowest heat of formation of all manganese oxides. Thus, Mn is reluctant to take the valence of the Ti atom it replaces; if it does, it would bind oxygen weakly since the heat of formation of β-MnO_2 is much lower than that of rutile TiO_2. This explains why Mn lowers the energy of oxygen vacancy formation more than the other metals, and it also explains why Mn does not want to bind an additional oxygen atom. The most stable tungsten oxide is WO_3, but rutile WO_2 is also formed. The energy of formation of WO_2 is so close to that of TiO_2 that, within the errors of experiment and DFT, the replacement of a Ti atom with a W atom does not change the formation energy of an oxygen vacancy.

This kind of correlation is not quantitative, but it may serve as a rough guide when trying to figure out which dopant is more likely to ease vacancy formation for a given host oxide.

5. The Energetics of CO Oxidation by $(MO)_xTi_{1-x}O_2$ (110) (M = V, Mo, Cr, or W) and $Mn_xTi_{1-x}O_2$ (110)

Doping with MO (M = V, Mo, Cr, or W) or with Mn makes it easier to make oxygen vacancies. This suggests that the doped oxide is a better oxidant than the undoped TiO_2. In what follows we examine the energies involved in steps 1−5 outlined in the introduction; we postpone for a future article the calculations of the activation energies.

When computing the energies of the intermediates in the reaction path we impose spin conservation. In other words, we avoid studying reactions the require spin "flipping" since they are very slow. One of the interesting findings is that for CO oxidation on $(MO)_xTi_{1-x}O_2$ (110) (M = Cr, Mo, or W) the initial state (spin and structure) is restored only after two catalytic cycles are completed.

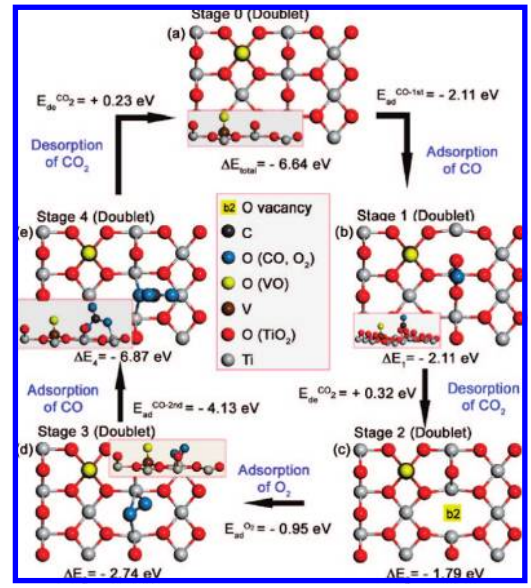

Figure 3. The structures and binding energies of the intermediates in CO oxidation on $(VO)_xTi_{1-x}O_2$ (110). The energy of initial state (doublet $(VO)_xTi_{1-x}O_2$ (110) plus the two CO molecules in the gas plus of an O_2 molecule in the gas) is taken to be zero. ΔE_x is the energy of the xth structure relative to that of the initial state; for example, ΔE_1 is the energy of CO adsorption on $(VO)_xTi_{1-x}O_2$ (110) (panel a) to form $(CO)_x(VO)_xTi_{1-x}O_2$ (110) (panel b), and ΔE_2 is the energy of CO_2 desorption from of $(CO)_x(VO)_xTi_{1-x}O_2$ (110) (panel b) to form $(VO)_xTi_{1-x}O_{2-\delta}$ (110) (Panel c). E_{ad}^{CO-1st}, $E_{de}^{CO_2}$−first, $E_{ad}^{O_2}$, $E_{ad}^{CO_2-2nd}$, and $E_{de}^{CO_2}$−second are the reaction energies for the first CO adsorption (from a to b), the first CO_2 desorption (from b to c), the adsorption of O_2 (from c to d), the second adsorption of CO (from d to e), and the second desorption of CO_2 (from e to a), respectively. The total energy ΔE_{tot} is the energy of the reaction of two CO molecules with one O_2 molecule to make two CO_2 molecules. This has been calculated from the energies of the steps in the cycle, and it is equal to the energy calculated for the gas phase reaction, as it should.

5.1. CO Oxidation by $(VO)_xTi_{1-x}O_2$ (110). Figure 3 shows the CO oxidation cycle rutile of TiO_2 (110) doped with V. We assume that the catalyst was prepared by doping to form $V_xTi_{1-x}O_2$ (110), and this was oxidized by prolonged exposure to O_2. This will convert the V atoms in the surface layer into VO, to form a material described by the formula $(VO)_xTi_{1-x}O_2$ (110). This has the lowest energy when $N_s = 1$ (doublet). In what follows, we take as the zero of the energy scale the energy of this doublet plus the energy of O_2(g) and CO(g).

Next we determine the binding site of CO to the surface. We find that the system has the lowest energy when CO binds (see Figure 3b) to two bridging oxygen atoms (denoted b1 and b2 in the right-hand panel in Figure 1) to form a "carbonate". We use for this compound the notation $(CO)_x(VO)_xTi_{1-x}O_2$ (110). The energy of formation of this compound from CO(g) and $(VO)_xTi_{1-x}O_2$ (110) is −2.11 eV. The negative sign means that the reaction is exothermic. CO is a singlet, and its adsorption does not change the spin of the supercell. Because of this, we use the energy of the doublet $(CO)_x(VO)_xTi_{1-x}O_2$ (110) to calculate the energy of CO adsorption (i.e., carbonate formation). CO does not react with the oxygen atom bound to vanadium. This V−O bond is similar to that in vanadyl, which is known to be a strong bond that is hard to break.

It costs 0.32 eV to remove CO_2 from $(CO)_x(VO)_xTi_{1-x}O_2$ (110). CO_2 removal creates an oxygen vacancy by removing the oxygen atom located at b2 (see Figure 3c and the right-

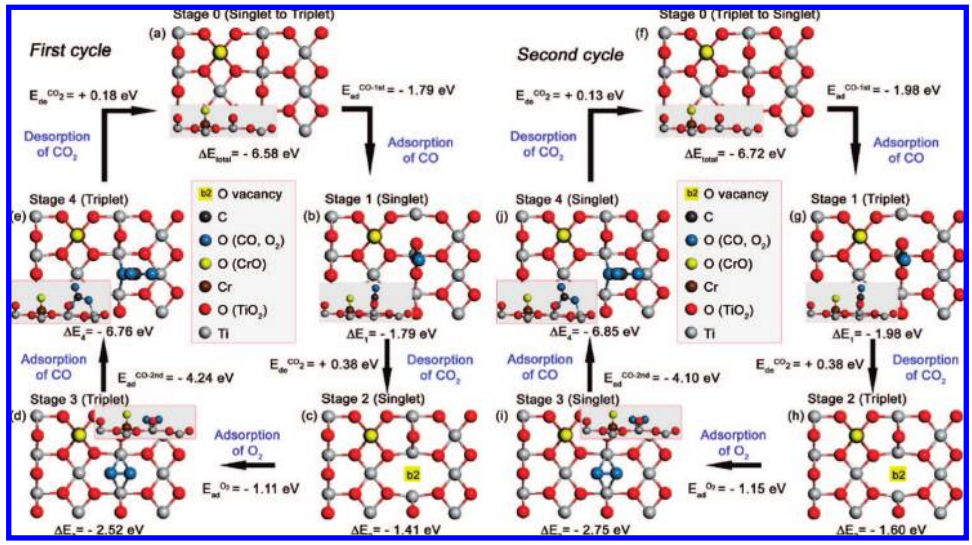

Figure 4. CO oxidation on $(CrO)_xTi_{1-x}O_2$ (110). This figure is organized similarly to Figure 3. The only difference is that one needs two cycles to recover the initial state of the catalyst; the catalyst starts as a singlet and ends up in a triplet state after the first cycle (panels a−e). A second cycle is needed to restore the catalyst to a singlet state.

hand-side panel in Figure 1), whose bond to the oxide is most weakened by the presence of the VO dopant. It takes more energy to desorb CO_2 by removing the oxygen atom at b1. We denote the compound formed after CO_2 removal by $(VO)_xTi_{1-x}O_{2-\delta}$ (110), where the subscript $2-\delta$ indicates the presence of an oxygen vacancy at b2 (see Figure 3c).

$(VO)_xTi_{1-x}O_{2-\delta}$ (110) reacts with gaseous oxygen, which binds to the oxygen vacancy. We denote the compound formed in this way by $(O_2)_x(VO)_xTi_{1-x}O_{2-\delta}$ (110). The adsorbed oxygen molecule is intact, and its position is shown in Figure 3d. This adsorbed oxygen molecule takes some electron charge from the vacancy (which is "electron rich"), and this weakens the O−O bond, as indicated by the fact that the bond of adsorbed O_2 is much longer than that of gas-phase O_2. Some of the electronic charge taken from the vacancy populates an antibonding orbital of O_2. $(VO)_xTi_{1-x}O_{2-\delta}$ (110) is a doublet ($S_1 = 1/2$), and oxygen is a triplet ($S_2 = 1$). The total spin of $(VO)_xTi_{1-x}O_{2-\delta}$ (110) + O_2(g) is therefore either $|S_1 - S_2| = 1/2$ or $S_1 + S_2 = 3/2$. Therefore, the formation of the doublet $(O_2)_x(VO)_xTi_{1-x}O_{2-\delta}$ (110) and the quartet $(O_2)_x(VO)_xTi_{1-x}O_{2-\delta}$ (110) are both spin allowed. We find that the doublet has the lowest energy and take this to be the more likely intermediate (this is true if the reaction is run at equilibrium and the entropy of the compounds does not play a substantial role). A study of the kinetics of this reaction system would have to calculate the activation energies for the formation of the doublet and of the quartet since they are both spin allowed.

The adsorbed oxygen in $(O_2)_x(VO)_xTi_{1-x}O_{2-\delta}$ (110), in the doublet state, reacts with CO to make a compound we denote $(CO_3)_x(VO)_xTi_{1-x}O_{2-\delta}$ (110), to indicate that a sort of carbonate has been formed at the vacancy site. This reaction is strongly exoergic, releasing 4.13 eV. Nevertheless, it is easy to remove CO_2 from the carbonate and leave behind an oxygen atom to heal the oxygen vacancy. At the end of this cycle we have consumed two CO molecules and an oxygen molecule to produce two CO_2 molecules and recover the catalyst (doublet $(VO)_xTi_{1-x}O_2$ (110)). It is important that the spin of the supercell at the end of the catalytic cycle is the same as the spin at the beginning of the cycle.

We note the similarity of this cycle with that of CO oxidation by $Au_xTi_{1-x}O_2$ (110).[48] The VO group does not participate in the CO oxidation cycle but helps it by weakening the bond of the oxygen atoms at b1 and b2 (see Figure 1) to the oxide. The energy of forming a vacancy at b2 in the case of $(VO)_xTi_{1-x}O_2$ (110) is 1.53 eV, whereas the same quantity for $Au_xTi_{1-x}O_2$ (110) is[48] 1.57 eV. The energy of CO adsorption on the b2 oxygen atom is −2.00 eV for $Au_xTi_{1-x}O_2$ (110), and it is −2.11 eV for CO adsorption on $(VO)_xTi_{1-x}O_2$ (110). The energy for desorbing CO_2 from $(CO)_x(VO)_xTi_{1-x}O_2$ (110) is 0.32 eV, and for $(CO)_xAu_xTi_{1-x}O_2$ (110) it is 0.21 eV. The only substantial difference between $(VO)_xTi_{1-x}O_2$ (110) and $Au_xTi_{1-x}O_2$ (110) is that the former adsorbs CO to make a carbonate (with the oxygens at b1 and b2) and the latter adsorbs CO perpendicular to the surface on top of the oxygen at b2.

Within a good approximation, doping TiO_2 (110) with VO is equivalent to doping with Au. This similarity is accidental; the properties of TiO_2 (110) doped with Cu, Ag, Ni, Pd, or Pt are quite different from those of TiO_2 (110) doped with Au. There are great changes in surface properties from one dopant to another.

5.2. CO Oxidation by $(CrO)_xTi_{1-x}O_2$ (110), $(MoO)_xTi_{1-x}O_2$ (110), and $(WO)_xTi_{1-x}O_2$ (110). The catalytic properties of these surfaces are similar to those of $(VO)_xTi_{1-x}O_2$ (110). There is, however, an interesting difference; it takes two catalytic cycles of surface reduction and reoxidation to return the surface of these catalysts to its initial state. Prior to CO adsorption the surface state is a singlet, but after the surface is reduced by CO and then is reoxidized by O_2 it is a triplet. Therefore, one reduction and reoxidation cycle does not return the surface to its initial state. It takes a second cycle of reduction and reoxidation to return the surface to the singlet state. The process is described in detail in Figure 4.

The lowest energy state of $(CrO)_xTi_{1-x}O_2$ (110) is a singlet (see Figure 4a). This adsorbs CO to form $(CO)_x(CrO)_xTi_{1-x}O_2$ (110) (see Figure 4b) and release 1.79 eV. Because CO is a singlet, we have calculated the adsorption energy using the energy of singlet $(CO)_x(CrO)_xTi_{1-x}O_2$ (110). It takes 0.38 eV to desorb CO_2 from this surface and leave an oxygen vacancy behind to form singlet $(CrO)_xTi_{1-x}O_{2-\delta}$ (110) (see Figure 4c). To heal the vacancy and return the surface to its initial state, we expose it O_2 to form $(O_2)_x(CrO)_xTi_{1-x}O_{2-\delta}$ (110) (see Figure 4d). Because the surface prior to O_2 adsorption is a singlet and O_2 is a triplet, the joint system is in a triplet state. Therefore, to calculate the energy of O_2

TABLE 4: The Reaction Energies for All the Steps in the Catalytic Cycle[a]

	reaction energy (eV)					
	E_{ad}^{CO-1st}	$E_{de}^{CO_2}$−first	$E_{ad}^{O_2}$	E_{ad}^{CO-2nd}	$E_{de}^{CO_2}$−second	ΔE_{total}
$(MoO)_xTi_{1-x}O_2$						
1st cycle	−0.71	+0.36	−1.11	−4.29	+0.18	−5.57
2nd cycle	−1.95	+0.34	−2.05	−4.29	+0.23	−7.72
$(WO)_xTi_{1-x}O_2$						
1st cycle	−0.22	+0.39	−1.32	−4.27	+0.20	−5.22
2nd cycle	−1.73	+0.38	−2.66	−4.28	+0.21	−8.08
$(CrO)_xTi_{1-x}O_2$						
1st cycle	−1.79	+0.38	−1.11	−4.24	+0.18	−6.58
2nd cycle	−1.98	+0.38	−1.15	−4.10	+0.13	−6.72
$(VO)_xTi_{1-x}O_2$	−2.11	+0.32	−0.95	−4.13	+0.23	−6.64
$Mn_xTi_{1-x}O_2$	−1.26	+0.25	−1.38	−4.44	+0.19	−6.64

[a] E_{ad}^{CO-1st} is the adsorption energy of CO, which binds to the oxygen atoms of the surface. $E_{de}^{CO_2}$–first is the energy of the release of CO_2 in the gas phase. $E_{ad}^{O_2}$ is the adsorption energy of O_2 at the vacancy site b2. E_{ad}^{CO-2nd} is the energy of CO reaction with the adsorbed O_2 to form a carbonate. $E_{de}^{CO_2}$−second is the energy of decomposition of this carbonate to release CO_2 in the gas phase and heal the oxygen vacancy. ΔE_{total} is the energy released by the complete cycle. For the systems that have two cycles each reaction occurs twice but with different spin states (see for example, Figure 4).

adsorption we use the energy of triplet $(O_2)_x(CrO)_xTi_{1-x}O_{2-\delta}$ (110). The adsorption of oxygen lowers the energy by 1.11 eV. The adsorption of O_2 at the vacancy site weakens the O−O bond, and this helps the molecule react with CO to form a carbonate that we denote by $(CO_3)_x(CrO)_xTi_{1-x}O_{2-\delta}$ (110) (see Figure 4e). This is a very exoergic reaction, producing 4.24 eV. The carbonate decomposes easily to liberate CO_2 (CO_2 removal energy is 0.18 eV) and heal the oxygen vacancy. This reaction leaves behind $(CrO)_xTi_{1-x}O_2$ (110) in a triplet state. We have started with singlet $(CrO)_xTi_{1-x}O_2$ (110) (Figure 4a) and used two CO molecules and one O_2 molecule to produce two CO_2 molecules and $(CrO)_xTi_{1-x}O_2$ (110), but at the end of this cycle the doped surface is in a triplet state. A second cycle is necessary (see the right-hand-side panel in Figure 4) to return the catalyst to a singlet $(CrO)_xTi_{1-x}O_2$ (110) and to generate a catalytic cycle in which the surface returns to its initial state. The steps in the second cycle are similar to the ones in the first cycle, but the spin states of the intermediates differ and so do the reaction energies.

A similar behavior is observed for CO oxidation on $(WO)_xTi_{1-x}O_2$ (110) and $(MoO)_xTi_{1-x}O_2$ (110). The reaction energies for these catalytic surfaces are given in Table 4. A comparison between all the catalysts studied here is made in Section 6.

5.3. CO Oxidation by $Mn_xTi_{1-x}O_2$ (110). In the presence of oxygen $Mn_xTi_{1-x}O_2$ (110) is more stable than $(MnO)_xTi_{1-x}O_2$ (110), and we study the catalytic activity of $Mn_xTi_{1-x}O_2$ (110). The results of the calculations of the most stable intermediates are shown in Figure 5. The lowest energy state of $Mn_xTi_{1-x}O_2$ (110) is a quartet. The steps in the catalytic cycle are very similar to that of previous systems. The only reaction we need to comment on is the adsorption of O_2 on the defective surface $Mn_xTi_{1-x}O_{2-\delta}$ (110). The state of $Mn_xTi_{1-x}O_{2-\delta}$ (110) is a quartet, and the oxygen is a triplet. The total spin can be a doublet, a quartet, or a sextet. The lowest energy of $(O_2)_x(Mn)_xTi_{1-x}O_{2-\delta}$ (110) is a quartet, and we assume that this is the state when the reaction is run at equilibrium.

6. A Comparison of the Catalysts

One of the goals of this study is to find out how much we can change the catalytic properties of an oxide by doping it and to find simple descriptors of the important steps in the

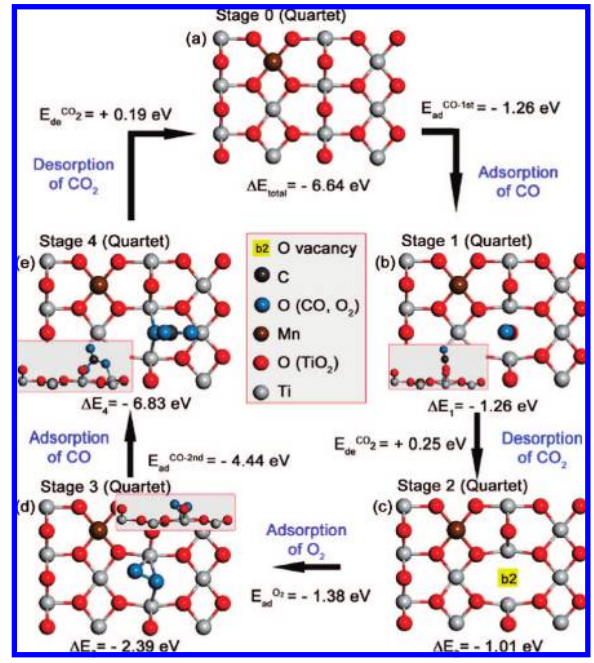

Figure 5. CO oxidation by $(Mn)_xTi_{1-x}O_2$ (110). This figure is organized similarly to Figure 3.

catalytic cycle. Because we are interested in oxidation reactions, we have examined only the catalytic properties of $(MO)_xTi_{1-x}O_2$ (110) (M = V, Cr, Mo, or W) and those of $Mn_xTi_{1-x}O_2$ (110), which are stable structures in the presence of oxygen. Because the oxidation takes place by a Mars−van Krevelen mechanism,[93] the energy of oxygen vacancy formation should be a good descriptor of the catalytic process. We can test if this is so. The intermediates and the reaction scheme for CO oxidation, for the catalysts examined here, are schematically shown in Figure 6. The energies of the intermediate reactions are collected in Table 4.

Note a remarkable thing: the desorption energies of CO_2 in steps 2 and 5 and the energy of the reaction of CO with the O_2 molecule adsorbed at the vacancy site (step 4) are independent of the catalyst. These quantities (i.e., *E*2, *E*4, and *E*5) do not change when we change the dopant or when we change the spin state of the surface (the reaction energies for 2, 4, and 5 in the first cycle are the same as those in the second cycle, even though the spin states differ). In the case of reaction 2 one would expect that if it is hard to make an

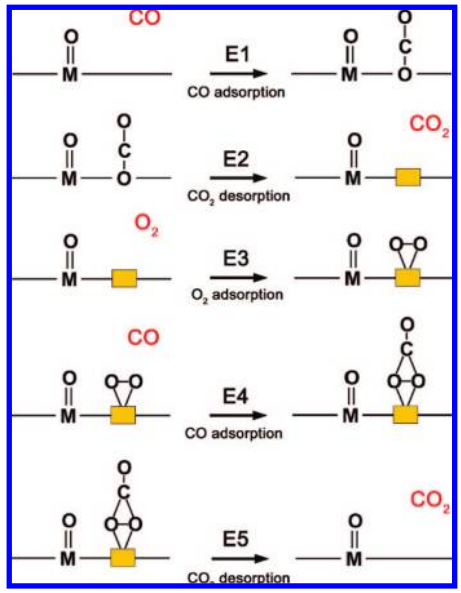

Figure 6. Schematic diagram of one cycle in CO oxidation by the doped TiO_2 system. M bound to O represents the dopant and the yellow box is the oxygen vacancy. The first reaction is CO adsorption and binding to the surface oxygen; the second is CO_2 desorption; the third is O_2 adsorption at the vacancy site; the fourth is the reaction of the adsorbed O_2 with CO to form a carbonate; and the fifth is the decomposition of the carbonate to produce CO_2 and recover the catalyst.

oxygen vacancy then it is hard to desorb CO_2 (since this process creates a vacancy at b2); this is not the case. One would also expect, perhaps naively, that a carbonate made at the site of an oxygen vacancy that is hard to make will be easier to decompose since more energy is gained by healing the oxygen vacancy; this is not the case either. Finally, one would think that an oxygen molecule adsorbed at the site of a vacancy that is hard to make will be more willing to react with CO since this may allow one of the oxygen atoms to heal the vacancy; the calculations show no such correlation. Thus, the energy of oxygen vacancy formation is not a good descriptor of the energies of carbonate decomposition to produce CO_2 or of the CO reaction with the O_2 adsorbed at a vacancy site.

The energy of vacancy formation is useful in characterizing the reaction of CO with the surface oxygen atoms. Figure 7a shows a linear dependence between CO adsorption energy and the energy ΔE_{v2} of vacancy formation at b2. The CO binding energy for catalysts that go through two cycles (i.e., $(MO)_xTi_{1-x}O_2$ (110), with M = Cr, Mo, or W) differs from one cycle to another (because the spin states are different), but they all fall on the straight line. The binding energy[48] of CO to the b2 site in $Au_xTi_{1-x}O_2$ (110) also falls on the line.

In Figure 7b we show that the binding energy of the O_2 molecule to the oxygen vacancy site at b2 is a linear function of ΔE_{v2}. For the systems in which CO oxidation takes place in two cycles we have used the average (the arithmetic mean) of the two O_2 adsorption energies.

This linearity exists because the desorption energies in the reactions 2, 4, and 5 are the same for all doped oxides. The energy of the CO adsorption reaction is given by eq 4,

$$E1 = E(\text{catCO}) - E(\text{cat}) - E(\text{CO}) \qquad (4)$$

where E(catCO) is the energy of the catalyst with CO bonded to the surface oxygen atoms, E(cat) is the energy of the catalyst without CO, and E(CO) is the energy of gas-phase CO. The

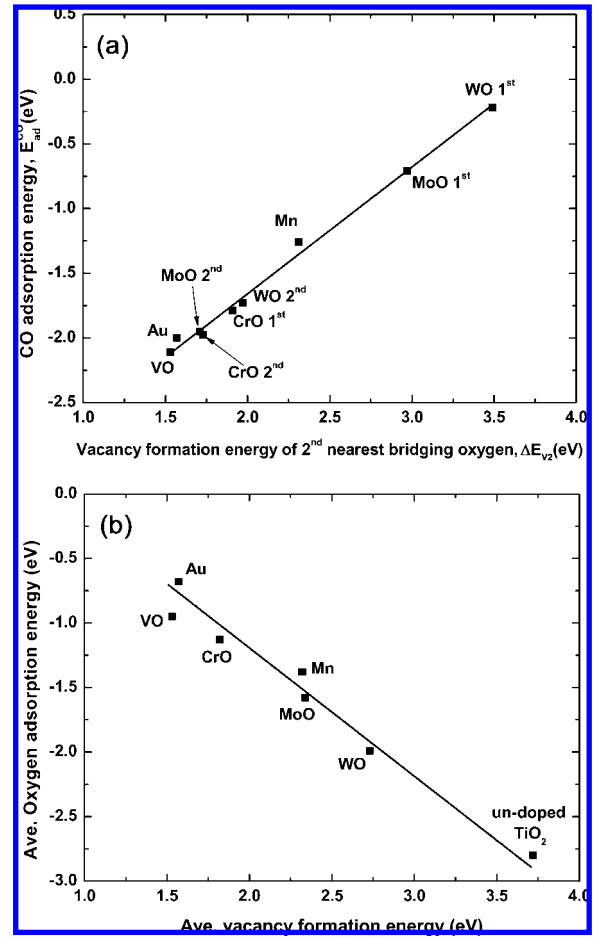

Figure 7. (a) The relationship between the energy of CO adsorption on the surface of the doped oxide and the energy of oxygen vacancy formation at the b2 site (see Figure 1 for definition). (b) The energy of oxygen adsorption at the oxygen vacancy site (the arithmetic average of the values in cycle 1 and 2) vs the energy of oxygen vacancy formation at the b2 site. The slopes are +1 and −1, respectively.

energy of CO_2 desorption caused by the decomposition of the carbonate formed at b1 and b2 is given by eq 5,

$$E2 = E(\text{CO}_2) + E(\text{catv}) - E(\text{catCO}) \qquad (5)$$

where E(catv) is the energy of the catalyst with an oxygen vacancy in b2 and $E(CO_2)$ is the energy of gas-phase CO_2. These equations are valid in either of the cycles. Adding eqs 4 and 5 gives eq 6,

$$E1 = \Delta E_{v2} + \Delta E(\text{CO}_2) - E_2 \qquad (6)$$

where ΔE_{v2} is the energy of formation of a vacancy in b2, and $\Delta E(CO_2)$ is the energy of formation of CO_2 in the gas phase. The term $\Delta E(CO_2) - E2$ in eq 6 is the same for all catalysts (see Table 4), which means that $E1$ depends linearly on ΔE_{v2}, as observed in Figure 7a. Inserting numerical values for $\Delta E(CO_2)$ and $E2$ gives eq 7,

$$E1 = \Delta E_{v2} - 3.65\ (\pm 0.07)\ \text{eV} \qquad (7)$$

which is consistent with the graph.

Figure 7b shows that the energy $E3$ of O_2 adsorption at the vacancy site b2 is also a linear function of the energy ΔE_{v2} of vacancy formation at the site b2, with a slope of 1. It is easy to show why this is so, in the case of a catalyst that needs only one oxidation cycle. If we add up the five reactions in the cycle, we obtain $2CO + O_2 = 2CO_2$. According to DFT, the energy

TABLE 5: Bader Charge of Dopant and Adsorbed Oxygen of $M_xTi_{1-x}O_2$ and $(MO)_xTi_{1-x}O_2$ Systems[a]

	dopant		the oxygen atom in MO	
Bader charge	first cycle	second cycle	first cycle	second cycle
$V_xTi_{1-x}O_2$	2.02			
$(VO)_xTi_{1-x}O_2$	2.18		−0.60	
$Cr_xTi_{1-x}O_2$	1.88			
$(CrO)_xTi_{1-x}O_2$	1.99	1.95	−0.44	−0.47
$Mo_xTi_{1-x}O_2$	2.30			
$(MoO)_xTi_{1-x}O_2$	2.72	2.48	−0.75	−0.78
$W_xTi_{1-x}O_2$	2.67			
$(WO)_xTi_{1-x}O_2$	2.98	2.94	−0.86	−0.86
$Mn_xTi_{1-x}O_2$	1.88			

[a] All dopants lost some amount of charge after making MO pre-structure.

TABLE 6: Bader Charge and Bond Length of Carbonate-like Adsorbed CO of Stage 1[a]

	Bader charge				bond length (Å)		
	C	O (CO)	b1	b2	C−O (CO)	C-b1	C-b2
$(VO)_xTi_{1-x}O_2$	4	−2.17	−1.71	−1.40	1.23	1.36	1.42
$(CrO)_xTi_{1-x}O_2$							
1st cycle	4	−2.17	−1.74	−1.36	1.24	1.35	1.42
2nd cycle	4	−2.17	−1.75	−1.35	1.24	1.35	1.42
$(MoO)_xTi_{1-x}O_2$							
1st cycle	4	−2.14	−1.75	−1.37	1.23	1.35	1.42
2nd cycle	4	−2.13	−1.76	−1.38	1.23	1.35	1.42
$(WO)_xTi_{1-x}O_2$							
1st cycle	4	−2.14	−1.75	−1.36	1.23	1.35	1.42
2nd cycle	4	−2.14	−1.75	−1.37	1.23	1.35	1.42
$Mn_xTi_{1-x}O_2$	4	−1.96		−2.04	1.20		1.21

[a] The adsorbed CO molecule makes a carbonate-like compound in V, Cr, Mo, and W-doped systems, whereas the adsorbed CO is converted to CO_2 in the Mn-doped system.

of this reaction is −6.65 eV. Therefore, the energies of the five steps satisfy eq 8 (this is essentially Hess's law from thermodynamics[90]).

$$E1 + E2 + E3 + E4 + E5 = -6.65\ (\text{eV}) \qquad (8)$$

Using eq 6 to replace $E1 + E2$ in eq 8 gives eq 9.

$$\Delta E_{v2} + E(CO_2) + E3 + E4 + E5 = -6.65\ (\text{eV}) \qquad (9)$$

All quantities in this equation, except for $E3$ (the energy of O_2 adsorption at the vacancy site) and ΔE_{v2} are independent of the catalyst. Therefore, we obtain a linear relationship between the energy $E3$ of O_2 adsorption at the vacancy site and that of vacancy formation at b2 (which is what Figure 7b gives).

Equation 8, on which this argument is based, is valid only for the systems involving one catalytic cycle. If the reaction mechanism involves two cycles, then the sum of all reaction energies is equal to twice −6.65 eV. We can start with this relationship and repeat the argument made above to conclude that the energy of vacancy formation is proportional with the arithmetic mean of the energies of oxygen adsorption in the first and the second cycle, as shown by Figure 7b.

It is often assumed that the amount of charge present on different atoms in the reaction intermediates is an important descriptor of the chemistry of the system. Because of this we have calculated the Bader charges on the atoms for different intermediates. The results are given in Tables 5 and 6. We find no correlation between the charges on different atoms in the system and their chemical activity.

7. Discussion

We have studied the energetics of the catalytic cycle for CO oxidation by rutile TiO_2 (110) doped with V, Cr, Mo, W, and Mn. Our calculations found that in the presence of gas phase oxygen all dopants, except Mn, bind an oxygen atom; therefore, the dopant is a MO group (M = V, Cr, Mo, or W).

On the basis of previous work we have assumed (and the present calculations confirm) that the dopant does not directly participate in the oxidation reaction; its role is to change the binding energy of the oxygen atoms in the surface layer to the oxide. An increase in this binding energy means that the doped oxide is a less-active oxidant in a reaction taking place by a Mars−van Krevelen mechanism. Such dopants would inhibit oxidation catalysis, but they may be useful in decreasing the loss of oxygen at high temperature. A dopant that decreases the energy of vacancy formation, on the other hand, will make the doped oxide a better oxidant than the undoped one. In previous work[56] we have found that doping ZnO with metal atoms having a higher valence than Zn will increase the energy of vacancy formation. Surprisingly, this is not the case for the systems studied here. Doping TiO_2 (110) with V, Cr, Mo, and Mn lowers the energy of vacancy formation, and doping with W leaves it practically unchanged. The energy of vacancy formation is lowered even more when V, Cr, W, or Mo bind an oxygen atom to form a MO group (which replaces a Ti atom at the surface of the oxide). The doped oxides studied here are better oxidants than rutile TiO_2 (110).

On the basis of the energies of various possible intermediates we propose the following reaction mechanism. (1) Because the dopants lower the energy of oxygen vacancy formation, the doped surface reacts more readily with CO, than the undoped one, to make a carbonate or a CO_2 molecule (for Mn dopant). (2) This decomposes to form CO_2 and leave behind an oxygen vacancy. (3) Oxygen from the gas phase is adsorbed at the vacancy site, and the O−O bond is weakened. (4) CO from gas phase reacts with the adsorbed oxygen to form a carbonate. (5) This easily decomposes to release CO_2, heal the oxygen vacancy, and restore the surface to its initial composition but not necessarily to its initial spin state. After one cycle of these five reactions, only $(VO)_xTiO_{2-x}$ (110) and $Mn_xTi_{1-x}O_2$ (110) return to the structure and the spin state they had before reacting with CO. In the case of $(CrO)_xTi_{1-x}O_2$ (110), $(WO)_xTi_{1-x}O_2$ (110), and $(MoO)_xTi_{1-x}O_2$ (110), the surface recovers its composition after the fifth reaction, but the spin state is different from the one it had before reacting with CO. For example, in the case of $(CrO)_xTi_{1-x}O_2$ (110), the surface is a singlet before CO is adsorbed and is a triplet after step 5 (see Figure 4). One more catalytic cycle is needed in order to restore the surface to the spin state it started with.

The energies of steps 2, 4, and 5 are independent of the composition of the spin state of the catalyst. This is very surprising since all three reactions involve either the formation or the annihilation of an oxygen vacancy, and the energy of vacancy formation does depend on catalyst composition and on its spin state (see Table 2). Thus, the catalysts are differentiated only through steps 1 and 3, which are the reaction of CO with the oxygen atoms b1 and b2 at the surface to form a carbonate (CO reacts with the Mn-doped surface to make a CO_2 molecule with the b2 oxygen atom) and through the adsorption of O_2 at the site of the oxygen vacancy at b2.

In previous work we have suggested that the energy of vacancy formation is likely to be a good descriptor of the catalytic cycle for oxidation by a Mars−van Krevelen mechanism. We find that, indeed, it is; the energies $E1$ and $E3$ (for

steps 1 and 3) are linear functions of the energy of formation of an oxygen vacancy at b2 (see Figure 7). Figure 7a shows that the easier it is to form an oxygen vacancy at b2, the higher the energy $E1$ of the reaction of CO with the surface. Figure 7b shows that the higher the energy of oxygen vacancy formation, the lower the energy $E3$ of oxygen adsorption at the vacancy site. That such correlation exists is not very surprising; it tells us that if a surface is easily reduced, then it is harder to reoxidize; it is, however, surprising to find a linear relationship. This result tells us that a doped oxide is a better catalyst (by a Mars−van Krevelen mechanism) than the undoped one if the dopant makes it easier to make oxygen vacancies, but not too easy. If ΔE_{v2} is very large, then the oxidation is very inefficient; if ΔE_{v2} is very small, then the oxide surface will be reduced too much, and its ability to oxidize CO (or other reducing agent) is substantially diminished. Qualitatively, a plot of activity versus ΔE_{v2} will be a volcano curve.

The three energies that change from one catalyst to another (the CO reaction with surface oxygen, the O_2 binding to the oxygen vacancy, and the energy of vacancy formation) are related by two linear relations. Therefore, any one of these three quantities can be used as a descriptor. They can be all computed with about the same difficulty. Experimentally, they are all hard to determine, mainly because we do not know the surface concentration of the dopant or of the oxygen vacancies. Nevertheless, efforts to measure one or all these quantities would be worthwhile.

When we calculated the energy of various intermediate reactions we have taken into account the total electronic spin state of the reactants and products. We included into the reaction mechanism only reactions in which the total electronic spin is conserved. To explain why we do this, let us examine a reaction in which compound A can change into a compound B that, in turn, can react and change into C, which desorbs and leaves the system. Let us assume A has the total electronic spin α and that B has several low energy states having the total electronic spin α, β, or γ. In addition, the low energy states of C have the total electronic spin states α and β. The energies of the other spin states of B and C are so large that we can ignore them as possible intermediates. If we are interested in thermodynamic equilibrium, then we should take into consideration only the states having the lowest energy, regardless of their spin. This is so because the system has an "infinite" time to reach equilibrium and therefore the spin−orbit coupling will manage to induce spin-forbidden transitions and bring each compound in the spin state having the lowest electronic energy. This is not necessarily true if we consider kinetics. If the reaction of A in a state with spin α to produce B with spin α, and that of B with spin α to produce C with spin α are reasonably fast, then the conversion of A with spin α to C with spin α will be much faster than any reaction that requires a change of spin. Therefore, A with spin α going into B with spin β or γ are bypassed and will not be part of the reaction mechanism. This is the reason why we study only the reactions that conserve spin; they are the only kinetically relevant states.

Although we have not calculated activation barriers, we can attempt to guess them from the reaction energies by using the Bronsted−Evans−Polany (BEP)[94,95] relationship. Norskov's group successfully used the BEP to predict the relative rates, of a given reaction, on different catalysts.[53,96,97] If we speculate that this relationship holds for the systems studied here, then we can make some guesses regarding the activity of these doped oxides. Table 4 shows that the energy of CO_2 desorption, by carbonate decomposition, and the energy of the reaction of CO with the adsorbed oxygen do not change when we change the catalyst; these reactions will not differentiate between catalysts. The catalysts will differ through their ability to adsorb CO on the surface and their ability to adsorb O_2 at an oxygen vacancy site. If we assume that, according to BEP, the larger the reaction energy the smaller the activation barrier, then we find that $(VO)_xTi_{1-x}O_2$ (110) is likely to be the fastest oxidant, whereas the reduced $Mn_xTi_{1-x}O_{2-\delta}$ (110) is the fastest oxygen adsorber. If we take into account both reactions, then we speculate that $(CrO)_xTi_{1-x}O_2$ (110), $(VO)_xTi_{1-x}O_2$ (110), and $Mn_xTi_{1-x}O_2$ (110) would be better CO oxidation catalysts than $(WO)_xTi_{1-x}O_2$ (110) and $(MoO)_xTi_{1-x}O_2$ (110).

The important steps in the catalytic cycle (the reactivity of surface oxygen and the ability of the vacancy to adsorb O_2) both depend on the energy of vacancy formation ΔE_{v2}. Because ΔE_{v2} is a property of the catalyst, we expect that catalysts that are good for CO catalytic oxidation would also be good for other catalytic oxidation reactions in which a reactant takes one oxygen atom from the surface. SO_2 oxidation to SO_3 is one reaction that comes to mind. These speculations will have to be tested by experiments or by future calculations of the activation energies.

Acknowledgment. We are grateful to the AFOSR for the Grant FAA9550-06-1-0167 that supported this research and to the PIRE-ECCI program at UCSB, supported by the National Science Foundation. Some of the calculations were performed using the facilities of the California Nano Systems Institute (CNSI), supported by NSF Grant No. CHE-0321368. H.Y.K. and H.M.L. are grateful to the HRHRP of KAIST.

References and Notes

(1) Cimino, A.; Bosco, R.; Indovina, V.; Schiavello, M. *J. Catal.* **1966**, *5*, 271.
(2) Cimino, A.; Sciavello, M.; Stone, F. S. *Discuss. Farad. Soc.* **1966**, *41*, 350.
(3) Krylov, O. V. *Catalysis by Non-Metals*; Academic Press: New York, 1970.
(4) Kiselev, V. F.; Krylov, O. V. *Adsorption and Catalysis on Transition Metals and Their Oxides*; Springer Verlag: Berlin, 1989.
(5) Cimino, A.; Stone, F. S. *Adv. Catal.* **2002**, *47*, 141.
(6) Deng, W.; De Jesus, J.; Saltsburg, H.; Flytzani-Stephanopoulos, M. *Appl. Catal., A* **2005**, *291*, 126.
(7) Fu, Q.; Deng, W.; Saltsburg, H.; Flytzani-Stephanopoulos, M. *Appl. Catal., B* **2005**, *56*, 57.
(8) Deng, W. L.; Flytzani-Stephanopoulos, M. *Angew. Chem., Int. Ed.* **2006**, *45*, 2285.
(9) Fu, Q.; Saltsburg, H.; Flytzani-Stephanopoulos, M. *Science* **2003**, *301*, 935.
(10) Guzman, J.; Carrettin, S.; Corma, A. *J. Am. Chem. Soc.* **2005**, *127*, 3286.
(11) Venezia, A. M.; Pantaleo, G.; Longo, A.; Di Carlo, G.; Casaletto, M. P.; Liotta, F. L.; Dganello, G. *J. Phys. Chem. B* **2005**, *109*, 2821.
(12) Carrettin, S.; Corma, A.; Iglesias, M.; Sanchez, F. *Appl. Catal., A* **2005**, *291*, 247.
(13) Calla, J. T.; Davis, R. J. *J. Phys. Chem. B* **2005**, *109*, 2307.
(14) Nishihata, Y.; Mizuki, J.; Akao, T.; Tanaka, H.; Uenishi, M.; Kimura, M.; Okamoto, T.; Hamada, N. *Nature* **2002**, *418*, 164.
(15) Tanaka, H.; Mizuno, N.; Misono, M. *Appl. Catal., A* **2003**, *244*, 371.
(16) Tanaka, H.; Tan, I.; Uenishi, M.; Kimura, M.; Dohmae, K. *Topics Cat* **2001**, *16/17*, 63.
(17) Tanaka, H.; Taniguchi, M.; Kajita, N.; Uenishi, M.; Tan, I.; Sato, N.; Narita, K.; Kimura, M. *Topics Cat* **2004**, *30/31*, 389.
(18) Baidya, T.; Gayen, A.; Hegde, M. S.; Ravishankar, N.; Dupont, L. *J. Phys. Chem. B* **2006**, *110*, 5262.
(19) Bera, P.; Malwadkarb, S.; Gayena, A.; Satyanarayanab, C. V. V.; Raob, B. S.; Hegde, M. S. *Catal. Lett.* **2004**, *96*, 213.
(20) Bera, P.; Gayen, A.; Hegde, M. S.; Lalla, N. P.; Spadaro, L.; Frusteri, F.; Arena, F. *J. Phys. Chem. B* **2003**, *107*, 6122.
(21) Bera, P.; Hegde, M. S. *Catal. Lett.* **2002**, *79*, 75.
(22) Perez-Alonso, F. J.; Melian-Cabrera, I.; Loper Granados, M.; Kapteijs, F.; Fierro, J. L. G. *J. Catal.* **2006**, *239*, 340.

(23) Nguyen, T. B.; Deloume, J. P.; Perrichon, V. *Appl. Catal., A* **2003**, *249*, 273.
(24) Nagaveni, K.; Hegde, M. S.; Madras, G. *J. Phys. Chem. B* **2004**, *108*, 20204.
(25) Shan, W.; Feng, Z.; Li, Z.; Zhang, J.; Shen, W.; Li, C. *J. Catal.* **2004**, *228*, 206.
(26) Olson, R. M.; Varganov, S.; Gordon, M. S.; Metiu, H.; Chretien, S.; Piecuch, P.; Kowalski, K.; Kucharski, S. A.; Musial, M. *J. Am. Chem. Soc.* **2005**, *127*, 1049.
(27) Wilkes, M. F.; Hayden, P.; Bhattacharya, A. K. *J. Catal.* **2003**, *219*, 295.
(28) Zamora, M.; Lopez, T.; Gomez, R.; Asomoza, M.; Melendez, R. *Catal. Today* **2005**, *289*, 107–108.
(29) Pino, L.; Recupero, V.; Benianati, S.; Shukla, A. K.; Hegde, M. S.; Bera, P. *Appl. Catal., A* **2002**, *225*, 63.
(30) Driscoll, D. J.; Lunsford, J. H. *J. Phys. Chem.* **1985**, *89*, 4415.
(31) Ito, T.; Lunsford, J. H. *Nature* **1985**, *314*, 721.
(32) Ito, T.; Wang, J. X.; Lin, C. H.; Lunsford, J. H. *J. Am. Chem. Soc.* **1985**, *107*, 5062.
(33) Lunsford, J. H. *Catal. Today* **1990**, *6*, 235.
(34) Lunsford, J. H. *Catal. Today* **2000**, *63*, 165.
(35) Shi, C.; Hatano, M.; Lunsford, J. H. *Catal. Today* **1992**, *13*, 191.
(36) Buyevskaya, O. V.; Wolf, D.; Baerns, M. *Catal. Today* **2000**, *62*, 91.
(37) Leveles, L.; Seshan, K.; Lercher, J. A.; Lefferts, L. *J. Catal.* **2003**, *218*, 296.
(38) Leveles, L.; Fuchs, S.; Seshan, K.; Lercher, J. A.; Lefferts, L. *Appl. Catal., A* **2002**, *227*, 287.
(39) Fuchs, S.; Leveles, L.; Seshan, K.; Lefferts, L.; Lemidou, A.; Lercher, J. A. *Topics Catal.* **2001**, *15*, 169.
(40) Trionfetti, C.; Babich, I.; Seshan, K.; Lefferts, L. *Topics Catal.* **2006**, *39*, 191.
(41) Trionfetti, C.; Babich, I. V.; Seshan, K.; Lefferts, L. *Appl. Catal., A* **2006**, *310*, 105.
(42) Berger, T.; Schuh, J.; Sterrer, M.; Diwald, O.; Knozinger, E. *J. Catal.* **2007**, *247*, 61.
(43) Gaab, S.; Find, J.; Muller, T. E.; Lercher, J. A. *Topics Catal.* **2007**, *46*, 101.
(44) Amin, N. A. S.; Pheng, S. E. *Chem. Eng. J.* **2006**, *116*, 187.
(45) Bera, P.; Priolkar, K. R.; Sarode, P. R.; Hegde, M. S.; Emura, S.; Kumashiro, R.; Lalla, N. P. *Chem. Mater.* **2002**, *14*, 3591.
(46) Gayen, A.; Priolkar, K. R.; Sarode, P. R.; Jayaram, V.; Hegde, M. S.; Subbanna, G. N.; Emura, S. *Chem. Mater.* **2004**, 16–2317.
(47) Zhao, S.; Gorte, R. J. *Appl. Catal., A* **2003**, *248*, 9.
(48) Chrètien, S.; Metiu, H. *Catal. Lett.* **2006**, *107*, 143.
(49) Shapovalov, V.; Metiu, H. *J. Catal.* **2007**, *245*, 205.
(50) Kustov, A. L.; Frey, A. M.; Larsen, K. E.; Johannessen, T.; Norskov, J. K.; Christensen, C. H. *Appl. Catal., A* **2007**, *320*, 98.
(51) Norskov, J. K.; Scheffler, M.; Toulhoat, H. *MRS Bulletin* **2006**, *31*, 669.
(52) Clausen, B. S.; Knudsen, K. G.; Nielsen, P. E. H.; Norskov, J. K. *Catal. Today* **2006**, *111*, 1.
(53) Norskov, J. K.; Bligaard, T.; Logadottir, A.; Bahn, S.; Hansen, L. B.; Bollinger, M.; Bengaard, H.; Hammer, B.; Sljivancanin, Z.; Mavrikakis, M.; Xu, Y.; Dahl, S.; Jacobsen, C. J. H. *J. Catal.* **2002**, *209*, 275.
(54) Greeley, J.; Norskov, J. K.; Mavrikakis, M. *Annu. Rev. Phys. Chem.* **2002**, *53*, 319.
(55) Chrètien, S. ; Metiu, H. unpublished, 2008.
(56) Pala, R. G. S.; Metiu, H. *J. Phys. Chem. C* **2007**, *111*, 8617.
(57) Ganduglia-Pirovano, M. V.; Hoffmann, A.; Sauer, J. *Surface Sci. Rep.* **2007**, *62*, 219.
(58) Pacchioni, G. *J. Chem. Phys.* **2008**, *128*, 182505.
(59) Di Valentin, C.; Pacchioni, G.; Selloni, A. *Phys. Rev. Lett.* **2006**, *art. no. 166803*, 97.
(60) Kresse, G.; Hafner, J. *Phys. Rev. B* **1993**, *47*, 558.
(61) Kresse, G.; Hafner, J. *Phys. Rev. B* **1994**, *49*, 14251.
(62) Kresse, G.; Furthmuller, J. *Phys. Rev. B* **1996**, *54*, 11169.
(63) Kresse, G.; Furthmuller, J. *Comput. Mater. Sci.* **1996**, *6*, 15.
(64) Perdew, J. P.; Wang, Y. *Phys. Rev.B* **1992**, *45*, 13244.
(65) Perdew, J. P.; Burke, K.; Wang, Y. *Physical Review B* **1996**, *54*, 16533.
(66) Vijay, A.; Mills, G.; Metiu, H. *J. Chem. Phys.* **2003**, *118*, 6536.
(67) Rasmussen, M. D.; Molina, L. M.; Hammer, B. *J. Chem. Phys.* **2004**, *120*, 988.
(68) Bredow, T.; Giordano, L.; Cinquini, F.; Pacchini, G. *Phys. Rev. B.* **2004**, *70*, 035419.
(69) Hameeuw, K. J.; Cantele, G.; Ninno, D.; Trani, F.; Iadonisi, G. *J. Chem. Phys.* **2006**, *124*, 024708.
(70) Thompson, S. J.; Lewis, S. P. *Phys. Rev. B* **2006**, *73*, 073403.
(71) Wigner, E.; Wittmer, E. E. *Z. Phys.* **1928**, *51*, 859.
(72) Carreon-Macedo, J. L.; Harvey, J. N. *J. Am. Chem. Soc.* **2004**, *126*, 5789.
(73) Harvey; J. N. DFT computation of relative spin-state energetics of transition metal compounds. In *Principles and Applications of Density Functional Theory in Inorganic Chemistry I*; Springer: Berlin/Heidelberg, 2004; Vol. 112, p 151.
(74) Harvey, J. N. *Faraday Discuss.* **2004**, *127*, 165.
(75) Harvey, J. N. *Phys. Chem. Chem. Phys.* **2007**, *9*, 331.
(76) Harvey, J. N.; Aschi, M. *Faraday Discuss.* **2003**, *124*, 129.
(77) Harvey, J. N.; Poli, R. *ACS Abstr.* **2003**, *226*, U433.
(78) Harvey, J. N.; Poli, R. *Dalton Trans.* **2003**, 4100.
(79) Harvey, J. N.; Poli, R.; Smith, K. M. *Coord. Chem. Rev.* **2003**, *238*, 347.
(80) Strickland, N.; Harvey, J. N. *J. Phys. Chem. B* **2007**, *111*, 841.
(81) Behler, J.; Delley, B.; Reuter, K.; Scheffler, M. *Phys. Rev. B* **2007**, *75*, 115409.
(82) Behler, J.; Delley, B.; Lorenz, B.; Reuter, K.; Scheffler, M. *Phys. Rev. Lett.* **2005**, *94*, 036104.
(83) Rozanska, X.; Fortrie, R.; Sauer, J. *J. Phys. Chem. C* **2007**, *111*, 6041.
(84) Chrètien, S.; Metiu, H. *J. Chem. Phys.* 2007.
(85) Tilocca, A.; Selloni, A. *ChemPhysChem* **2005**, *6*, 1911.
(86) Matthey, D.; Wang, J. G.; Wendt, S.; Matthiesen, J.; Schaub, R.; Laesgsgaard, E.; Hammer, B.; Besenbacher, F. *Science* **2007**, *315*, 1692.
(87) Epling, W. S.; Peden, C. H. F.; Henderson, M. A.; Diebold, U. *Surf. Sci.* **1998**, *333*, 412–413.
(88) Bader, R. *Atoms in Molecules: A Quantum Theory*; Clarendon: Oxford, 1994.
(89) Henkelman, G.; Arnaldsson, A.; Jonsson, H. *Comput. Mater. Sci.* **2006**, *36*, 354.
(90) Metiu, H. *Physical Chemistry: Thermodynamics*; Taylor and Francis Group: New York, 2006.
(91) Metiu, H. *Physical Chemistry: Statistical Mechanics*; Francis and Taylor Group: New York, 2006.
(92) Samsonov, G. V. *The Oxide Handbook*; Plenum: New York, 1973.
(93) Mars, P.; van Krevelen, D. W. *Chem. Eng. Sci. Spec. Suppl.* **1954**, *3*, 41.
(94) Bronsted, N. *Chem. Rev.* **1928**, *5*, 231.
(95) Evans, M. G.; Polanyi, M. *Trans. Farad. Soc.* **1938**, *34*, 11.
(96) Logadottir, A.; Rod, T. H.; Nørskov, J. K.; Hammer, B.; Dahl, S.; Jacobsen, C. J. H. *J. Catal.* **2001**, *197*, 229.
(97) Christensen, C. H.; Norskov, J. K. *J. Chem. Phys.* **2008**, *128*, 182503.

JP802296G